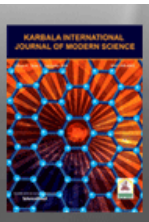

Karbala International Journal of Modern Science

Volume 11 | Issue 1 Article 1

Exfoliated Hydrotalcite-Transition Metal Complex Composite for Eco-Friendly and Efficient Catalytic Degradation of 4-Nitrophenol

Sidra Khan
National Centre of Excellence in Analytical Chemistry, University of Sindh, Jamshoro-Pakistan.

Najma Memon
National Centre of Excellence in Analytical Chemistry, University of Sindh, Jamshoro-Pakistan, najma.memon@usindh.edu.pk

Saima Q. Memon
M.A. Kazi Institute of Chemistry, University of Sindh, Jamshoro-Pakistan.

Yilmaz Yurekli
Bioengineering Department Engineering Faculty, Manisa Celal Bayar University, Yunusemre, 45140, Manisa, Turkey

Exfoliated Hydrotalcite-Transition Metal Complex Composite for Eco-Friendly and Efficient Catalytic Degradation of 4-Nitrophenol

Abstract

Nitrophenols are notorious aquatic organic contaminants found as degradation products of various parent compounds, including pesticides and industrial chemicals that persist in the environment and must be removed. Catalytic degradation is one of the feasible routes to clean the contaminated water systems, however, environmental contamination with catalysts is also widespread. Herein, we report an environmentally friendly catalyst based on composited Fe-Schiff's base with exfoliated layered double hydroxides (LDH) of aluminum and nickel (hydrotalcite). The composite showed agglomerated pleated LDH structures sheathed with Fe(III)SB. Nitrogen adsorption isotherm data exhibited improved surface area and narrow pores patterns for composite as compared to LDH indicating Fe(III) SB-induced change in the morphology of LDH. Also, significant improvement in catalytic efficiency was observed for Fe(III)SB-LDH over pristine LDH. 4-nitrophenol (10 mg/L) degradation of 99% in five minutes was achieved at pH 6 using a catalyst-to-volume ratio of 1:20 and 20 mM H_2O_2 as oxidant. It is concluded that phenomenal improvement in catalyst efficiency can be attributed to Fe-Schiff's base modification.

Keywords

: Environmental impact; Fe-Schiff's base composites; Aluminum and nickel hydrotalcite; Heterogeneous catalytic efficiency

RESEARCH PAPER

Exfoliated Hydrotalcite-transition Metal Complex Composite for Eco-friendly and Efficient Catalytic Degradation of 4-nitrophenol

Sidra Khan [a], Najma Memon [a,*], Saima Q. Memon [b], Yilmaz Yurekli [c]

[a] National Centre of Excellence in Analytical Chemistry, University of Sindh, Jamshoro, Pakistan
[b] M.A. Kazi Institute of Chemistry, University of Sindh, Jamshoro, Pakistan
[c] Bioengineering Department Engineering Faculty, Manisa Celal Bayar University, Yunusemre, 45140 Manisa, Turkey

Abstract

Nitrophenols are notorious aquatic organic contaminants found as degradation products of various parent compounds, including pesticides and industrial chemicals that persist in the environment and must be removed. Catalytic degradation is one of the feasible routes to clean the contaminated water systems, however, environmental contamination with catalysts is also widespread. Herein, we report an environmentally friendly catalyst based on composited Fe-Schiff's base with exfoliated layered double hydroxides (LDH) of aluminum and nickel (hydrotalcite). The composite showed agglomerated pleated LDH structures sheathed with Fe(III)SB. Nitrogen adsorption isotherm data exhibited improved surface area and narrow pores patterns for composite as compared to LDH indicating Fe(III) SB-induced change in the morphology of LDH. Also, significant improvement in catalytic efficiency was observed for Fe(III)SB-LDH over pristine LDH. 4-nitrophenol (10 mg/L) degradation of 99% in 5 min was achieved at pH 6 using a catalyst-to-volume ratio of 1:20 and 20 mM H_2O_2 as oxidant. It is concluded that phenomenal improvement in catalyst efficiency can be attributed to Fe-Schiff's base modification.

Keywords: Environmental impact, Fe-Schiff's base composites, Aluminum and nickel hydrotalcite, Heterogeneous catalytic efficiency

1. Introduction

Layered double hydroxides (LDHs) are two-dimensional (2D) layered materials, trending in current research with diversified applications, such as the removal of dyes and phenols from wastewater [1]. The use of LDHs for the degradation of dyes and 4-nitrophenol can be considered sustainable in multiple ways. Firstly, LDHs are non-toxic and have a low environmental impact compared to traditional chemical methods of water treatment. Secondly, LDHs have a high adsorption capacity for pollutants, which means they can effectively remove dyes and 4-nitrophenol from water with relatively small amounts of the material. This can help to reduce the overall cost of water treatment. Thirdly, LDHs can be regenerated and reused multiple times, which further reduces the cost of treatment and reduces the need for additional materials. Lastly, LDHs can be synthesized from natural resources such as clay minerals, which are abundant and widely available. This can make the production of LDHs more sustainable than the production of other types of water treatment materials. LDHs for the degradation of 4-nitrophenol is an environmentally friendly and sustainable way of water treatment. As LDHs are layered materials and exhibit space between their layers, hence they are found to be a host for incorporation of planar transition metal complex catalysts including Schiff's base, phthalocynine, or porphyrin [2–6]. Aside from the effectiveness of modified LDHs, these can also serve as heterogeneous materials in an aqueous environment, providing an added benefit for use in sustainable

Received 13 August 2024; revised 18 November 2024; accepted 21 November 2024.
Available online 12 December 2024

* Corresponding author.
E-mail address: najma.memon@usindh.edu.pk (N. Memon).

https://doi.org/10.33640/2405-609X.3383

environmental development [7]. There are extensive studies dealing with the immobilization of catalyst complexes within mesoporous layers. However, the incorporation of transition metal complexes into hydrotalcite layers has garnered little attention. It is claimed that LDH-hosted catalyst doesn't leach and can be reused several times without loss of activity [8,9]. In the past few years, composited Schiff's bases have been reported because of its easy production. Schiff's bases, which are produced from amine and aldehyde which also function as transition metal complexes, have also been used to modify LDH. Schiff's base complexes of transition metal ions such as cobalt, nickel, copper, zinc, iron, manganese, chromium, etc. can catalyze the polymerization of olefins, the ring opening polymerization of cycloalkenes, the oxidation of hydrocarbons, the ring opening of large cycloalkanes, the metathesis of olefins, the reduction of ketones, the alkylation of allylic substrates, the hydrosilation of olefins, the Michael addition reaction and the heteroannulation reaction [10]. K.M. Parida *et al.* synthesized Fe(III)-Schiff's base and immobilized it on LDH, which is a heterogeneous catalyst. The LDH immobilized with Fe(III)-Schiff's base showed good catalytic activity for cyclohexane by using an oxidizing agent (H_2O_2) [3]. They used sodium salt of 2-aminonicotinic acid and salicylaldehyde to prepare Schiff's base and incorporated it into Zn–Al-based LDH.

In our study, we have prepared Fe(III)-Schiff's base (benzophenone and 2-aminothiophenol) complex and used it to modify LDH (Ni/Al) for surface functionalities and morphological features. LDH was exfoliated into layers using the formamide method. To assess the efficiency of prepared materials, H_2O_2-driven oxidation of 4-nitrophenol using a newly developed catalyst was conducted. Nitrophenols are among the toxic and carcinogenic pollutants that are produced during many industrial and agricultural activities, henceforth reactions that can remove these compounds are of crucial importance. This paper reports on the synthesis and characterization of catalysts, parametric optimization for catalytic oxidation of nitrophenol, and identification of degradation products.

2. Experimental

2.1. Material

Aluminum (III) nitrate [$Al(NO_3)_3.9H_2O$], nickel (II) nitrate [$Ni(NO_3)_2.6H_2O$], Iron (III) nitrate nonahydrate [$Fe(NO_3)_3 \cdot 9H_2O$], benzophenone, and 2-aminothiophenol were purchased from Sigma Aldrich. All solvents used were of analytical grade. The stock solution of 1000 mg/L concentration of 4-nitrophenol (4-NP) ($C_6H_5NO_3$) was prepared and diluted to the required concentrations by using DI water.

2.2. Synthesis of Ni–Al LDH and Fe(III)/Schiff's base (Fe(III)/SB)

In the general procedure, the nitrate salts of Ni^{2+} 5.48 g (3 mM) and Al^{3+} 2.12 g (1 mM) in a ratio of 3:1 were added dropwise to the solution of NaOH 4.0 g (1.0 M) with continuous stirring at 60 °C under nitrogen environment. The resultant slurry was kept at 60 °C overnight, then it was filtered and washed through DI water and dried.

For the preparation of Schiff's base, the equimolar solution of benzophenone 0.0911g/25 mL (20 mM) and 2-aminothiophenol 8.3375mL/25 mL (20 mM) in ethanol were refluxed for 3h. The obtained crystals were recrystallized. Fe(III)-2-aminothiophenol-benzophenone complex was prepared by stirring ethanoic solution of 0.001M of Schiff's base 0.001M of $Fe(NO_3)_3 \cdot 9H_2O$ for 1h at room temperature. The precipitates obtained were washed, dried, and stored for further use.

2.3. Modification of Fe(III)/SB-LDH

Exfoliation was carried out by suspending Ni–Al LDH (0.57g) in formamide (30 g) for 24 h. Ethanoic solution of Fe(III)-2-aminothiophenol-benzophenone complex (3 g in 50 mL) was prepared. The two solutions were mixed and stirred for 24 h at room temperature followed by 48h at 70 °C. Then the mixture was cooled at room temperature and the precipitates were filtered and washed with ethanol.

2.3.1. Contaminants degradation at the bench level

Batch experiments for degradation of 4-nitrophenol were conducted in 15 mL glass bottles in a shaker bath at 30 °C. The reaction suspension was prepared by mixing H_2O_2 (20 mM), LDH or Fe(III) SB-LDH (0.025 g), and 5 mL of 4-nitrophenol (4-NP) (10 mg/L). The sample was withdrawn in 10 min, filtered immediately with cellulose filter paper (0.2 μm), and analyzed. Experiments were conducted at different pH; the initial pHs of 4-NP solutions were adjusted with 0.1M NaOH or 0.1M HCl for parametric optimization studies. All the reactions were carried at the initial pH of the solution and pH after addition of other reactants was not recorded.

To evaluate the reusability of Fe(III)SB-LDH, the experiment was carried out in a 100 mL glass bottle with 3.0 g of Fe(III)SB-LDH at a temperature of 30 °C. The experimental mixture was prepared by combining 25 mL of 4-nitrophenol solution (10 mg/L)

with 25 mL of H_2O_2 solution (20 mM). The initial pH of the solution was measured to be 6.0, and as this value was deemed suitable for the desired reaction conditions, no further addition of acid or base was required. The reaction proceeded without any subsequent pH adjustments. This mixture was then placed in a shaker for 10 min. After shaking, the mixture was filtered, and the catalyst was subsequently dried and weighed. The entire procedure was repeated four times.

2.3.2. Determination of degradation products

The qualitative analysis of degradation products was analyzed on high-performance liquid chromatography (HPLC) (Thermo Scientific ultimate 3000) equipped with a C18 (150 mm × 4.6 mm, 3 μm) and a diode-array detector (DAD). The methanol and water (70:30, v/v) was used as mobile phase at a constant flow rate of 1 mL/min, the column temperature was 40 °C. The detection wavelength was 320 nm for nitrophenol whereas a 3D diode-array scan was used to identify peak maxima and UV–Vis spectra for degradation products.

2.4. Characterization technique of Ni/Al-LDH and Fe(III)/SB-LDH

LDH and Fe(III)SB-LDH were characterized by different techniques such as Fourier transform infrared spectroscopy (Thermo Scientific Nicolet TM iS10) to determine the functional groups of the material using a wavenumber of 400–4000 cm^{-1} under ATR mode. Scanning electron microscopy (SEM) and X-ray diffraction analysis (XRD) were performed by Bruker-D2 phaser diffractometer, with CuKa radiation (λ = 1.5418 Å) with an operating voltage of 30 kV and operating current of 10 mA. The Brunauer–Emmett–Teller (BET) analysis was used to determine the surface area and pore size of the prepared material (Autosorb-1 Quantachrome, AsimQwin). Samples were degassed under vacuum at 150 °C for 24 h before the measurement. The pore size distribution of prepared material was determined by the BJH (Barrett–Joyner–Halenda) model. Determination of 4-nitrophenol for parametric optimization was conducted by a double-beam UV–visible spectrophotometer (Agilent carry 100).

3. Results and discussion

3.1. Catalyst characterization

3.1.1. Functional group determination

FT-IR spectra of Fe(III)SB, and Fe(III)SB-LDH are shown in Fig. 1.

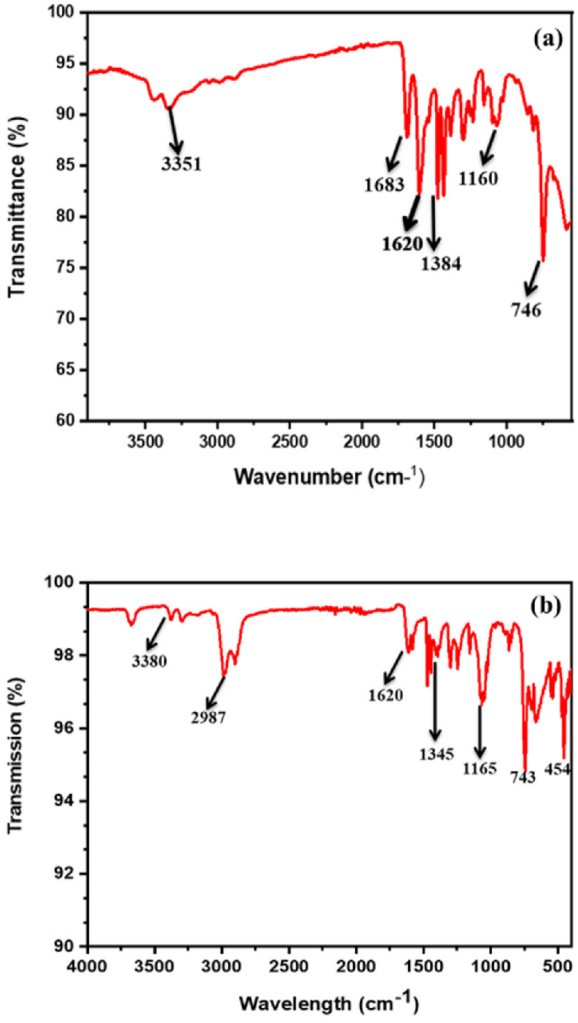

Fig. 1. FT-IR spectra of (a) Fe(III)SB (b) Fe(III)SB-LDH.

In the spectrum of Fe(III)SB (Fig. 1a), the characteristic band at 1620 cm-1 shows stretching due to C=N of the imine group, 1683 cm^{-1} for C=O stretching, 1384 for free nitrate ions, and 3351 due to the presence of water molecules [11,12]. The 1384 cm^{-1} absorption band due to stretching of NO_3^- in Fe(III)SB modified LDH spectrum (Fig. 1b) shifted to higher wavelength in Fe(III)SB-LDH of 1395 cm^{-1} [13]. The band at 2987 cm^{-1} in Fe(III)SB-LDH is due to CH stretch. In LDH the bands at 450 cm^{-1} and 664 cm^{-1} can be attributed to O-M-O and MOH stretching respectively [14]. The bands in Fe(III)SB-LDH shifted to higher wavelength *i.e.*, 454 cm^{-1} and 743 cm^{-1} after incorporation of Fe(III) SB in LDH. The spectral bands observed at frequencies lower than 750 cm^{-1} are associated with lattice vibration modes that correspond to M–O (M = Al, Ni) in the LDH sheets [15].

3.2. Surface morphology

SEM images of LDH and Fe(III)SB-LDH are shown in Fig. 2. The SEM images (Fig. 2) of pure Ni/Al-LDH suggest the formation of agglomerated structures that overlap or pleated with each other. It resembles earlier reported structures of LDHs [16]. The topography of Fe(III)SB-LDH (Fig. 2) shows the agglomerated pleated LDH layers are sheathed with Fe(III)SB. The results indicate successful compositing of the two materials.

3.2.1. Crystal structure

The diffractogram, shown in Fig. 3, depicts that Ni–Al LDH has main hydrotalcite peaks that appeared at 2Θ equal to 11.20, 22.68, 29.06, 35.06, 38.42, 44.71 and 60.66 equivalents to (003), (006), (101), (009), (012), (015) and (018) diffraction planes, respectively. These peaks show that the material is a crystalline, layered structure with rhombohedral symmetry and represent all the reflections reported by Wang *et al.* [17]. However, the intensity of peaks varies which in turn depends upon the synthesis process and post-treatment. For example, a paper

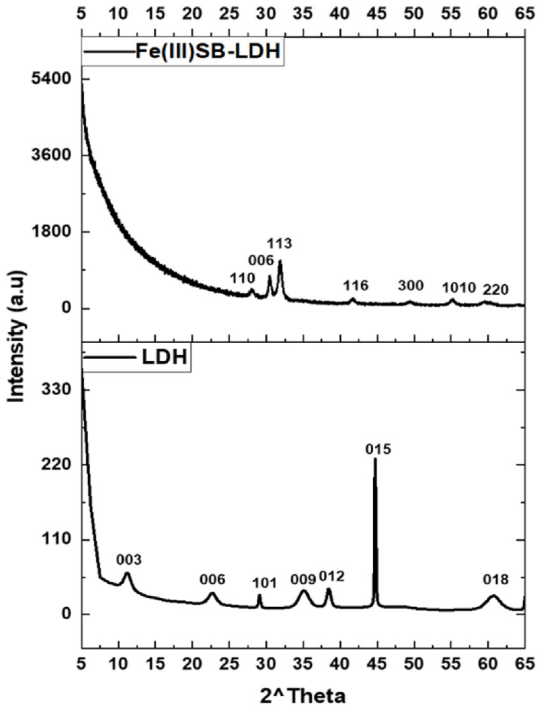

Fig. 3. XRD diffractogram of LDH and Fe(III)SB-LDH.

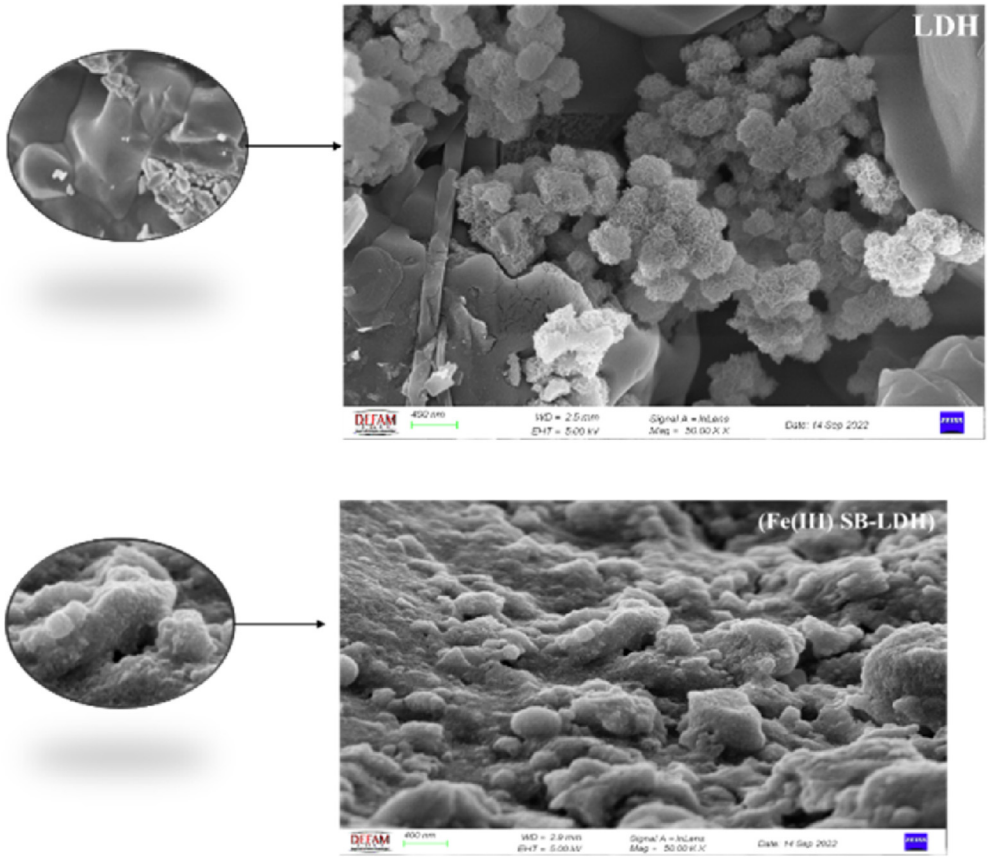

Fig. 2. SEM images of Al–Ni LDH (A) and Fe(III)SB-LDH (B).

[18] reports Al–Ni LDH where reflections are observed at characteristics 2θ values but a reflection (003) at 2θ value of 11.20 was the only intense peak. This suggests that Ni–Al LDH can represent reflections with variable intensity. Hence it confirms that the synthesized material under this study is Ni–Al LDH. Furthermore, the peak appears at 2θ of 29.06 with a diffraction plane of 101 does not relate with LDH reflections, may be attributed to the presence of NiO [19]. However, peaks for Fe(III)SB-LDH appear at 2Θ equals to 27.99, 30.43, 31.86, 41.91, 49.39, 55.25, and 59.89 equivalents to (110), (006), (113), (116), (300), (1010), and (220) which is significantly different then pristine LDH. This may be explained that during exfoliation using formamide and heat treatment (70 °C) for 72h, it is observed that the (003) moves to greater angles, indicating a decrease in the interlamellar space [20] and other peaks diminished. This confirms that the LDH exfoliated phase agglomerated with Fe-SB and lost its ordered layered structure. This kind of behavior is reported in literature. Usually, there are two types of nanocomposites depending upon the dispersion of clay particles. The first type is an intercalated guest substance/clay nanocomposite, which consists of well-ordered clay multilayers. In these nanocomposite samples, the extent of guest penetration is not sufficient to delaminate the ordered structures and guest substances reside in layers. The second type is an exfoliated guest substance/clay nanocomposite, in which there is a loss of ordered structure due to the extensive penetration of guest substance into the layers [21]. In this study, LDH forms an exfoliated nanocomposite with Fe-SB resulting in the loss of layered structure as evidenced by XRD of composite. This aggregated behavior is also supported by SEM images (Fig. 2).

The miller indices (hkl) values (Table-1) were determined utilizing X'Pert HighScore plus. The basal d-spacing value decreases from 7.89 Å for LDH and 3.18 Å, respectively. Basal spacing is calculated by Bragg's equation.

$$d = \frac{\lambda}{2 \sin \theta}$$

Here, d is basal spacing, θ is the diffraction angle, and λ is the wavelength.

3.2.2. Porosity measurements

N_2 adsorption–desorption isotherms of Ni/Al LDH at 77K are explained in Fig. 4 (a) and (b).

LDH shows typical type II isotherm with H3 hysteresis loop as described by IUPAC classification [22]. This type of isotherms is given by non-rigid aggregates of plate-like particles (e.g., certain clays) but also if the pore network consists of macropores that are not filled with pore condensate. A similar type of pore structure is reported earlier, mentioning that inter-lamellar pores are not assessable by nitrogen. The porosity obtained by nitrogen adsorption porosimetry explains external pores only [23]. However, Fe(III)SB-LDH shows merged two types of isotherm. The first half of the isotherm resembles the H4 hysteresis loop whereas the second half indicates the H5 hysteresis loop pattern. H4 indicates the filling of micropores in the aggregated crystals whereas H5 is associated with certain pore structures containing both open and partially blocked mesopores. Furthermore, BJH pore size distribution desorption curves for the two materials were also different. The change in isotherm pattern indicates that Fe(III)SB induces a significant change in the morphology of LDH as evidenced by improved surface area and narrow pores, therefore the composite is expected to behave differently.

Table 1. The XRD data of LDH and Fe(III)SB-LDH.

Peak position	Diffraction plane value (hkl)			Compound	Basal spacing with adjacent peak (Å)
	h	k	l		
11.20	0	0	3	LDH	7.89
22.68	0	0	6	LDH	3.91
27.99	1	1	0	Fe(III)SB-LDH	3.18
29.06	1	0	1	LDH	3.07
30.46	0	0	6	Fe(III)SB-LDH	2.93
31.87	1	1	3	Fe(III)SB-LDH	2.80
35.06	0	0	9	LDH	2.55
38.42	0	1	2	LDH	2.34
41.91	1	1	6	Fe(III)SB-LDH	2.15
44.71	0	1	5	LDH	2.02
49.395	3	0	0	Fe(III)SB-LDH	1.84
55.255	1	0	10	Fe(III)SB-LDH	1.66
59.89	2	2	0	Fe(III)SB-LDH	1.54
60.66	0	1	8	LDH	1.52

The porous properties and surface area of the material are summarized in Table-2 and Fig. 5. It is seen that the MBET surface area and pore volume of LDH is 3.05 m^2/g and 0.007 cc/g, respectively. The MBET surface area and pore volume of Fe(III)SB-LDH were 6.561 m^2/g and 0.003 cc/g. A decrease in pore diameter and pore volume is attributed to the possibility of incorporation of Fe(III)-Schiff's base into LDH while the surface area increases.

3.2.3. Thermogravimetric analysis (TGA)

TGA analysis confirms the modification of LDH to Fe(III)SB-LDH as shown in Fig. 6. In the TGA curve, the weight loss was 11.45% below 200 °C for LDH whereas for Fe(III)SB-LDH it was 27.61% which may be related to the loss of physiosorbed water molecules and alcohol moieties on the surfaces of LDH

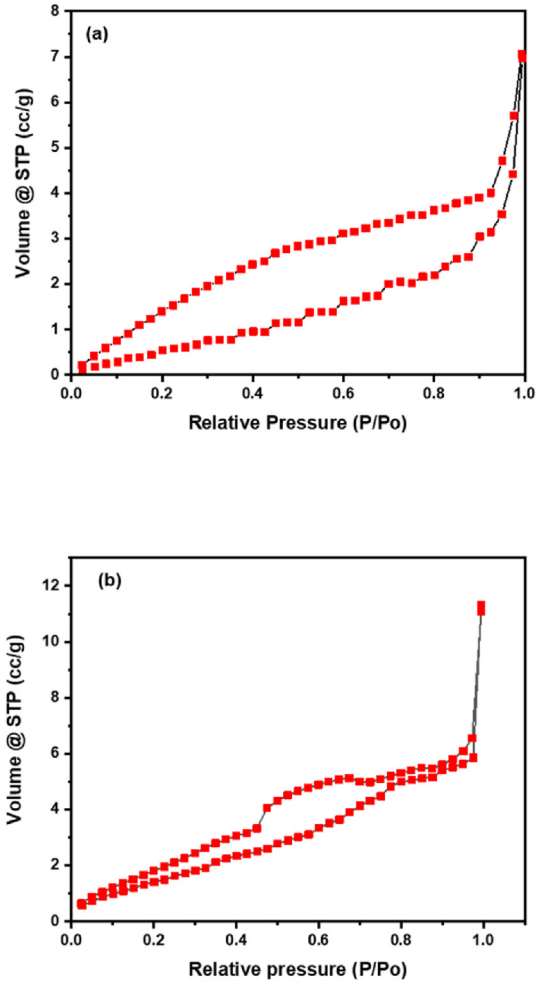

Fig. 4. N_2 adsorption–desorption isotherm (a) LDH and (b) Fe(III)SB-LDH.

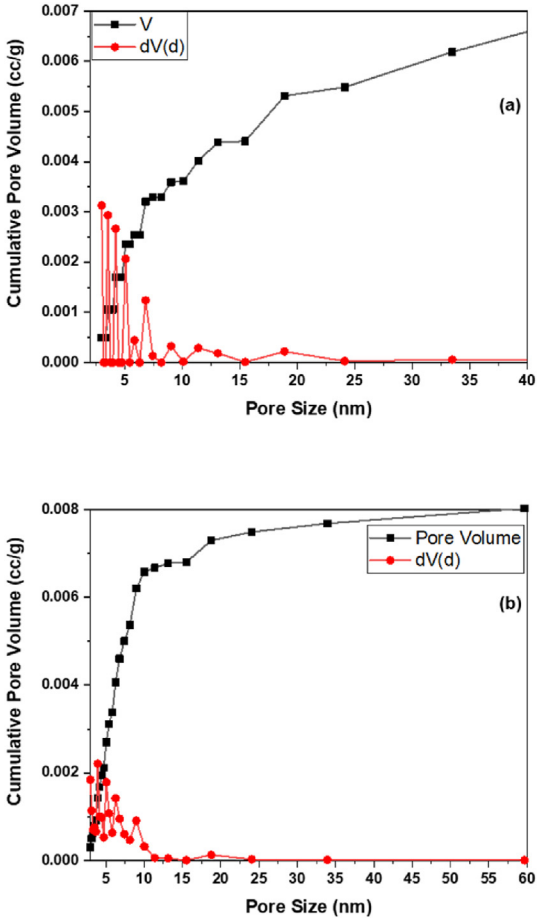

Fig. 5. N_2 adsorption porosimetry data. a) LDH and b) Fe(III)SB-LDH Graph between cumulative pore volume vs pore size.

and Fe(III) Schiff's base modified LDH. The weight loss of 21.4% and 22.39% was observed for LDH and Fe(III)SB-LDH, respectively in the temperature range of 200–300 °C which are ascribed to the elimination of acid dopant [24,25]. The third weight loss process starts at around 450 °C, and it is attributed to the thermal decomposition of LDH (7.97%) and Fe(III)SB-LDH (9.233) [26].

3.3. Application of Fe(III)SB-LDH catalyst for oxidative removal of 4-nitrophenol

Oxidation of 4-nitrophenol using H_2O_2 is reported which is influenced by chemical conditions of the reaction medium. The influencing factors for the oxidation of 4-nitrophenol are pH, catalyst dose, concentration of 4-nitrophenol, and reaction time, which are studied. The findings suggest that 99% of 4-nitrophenol (10 mg/L) degrades at a pH value of 6 and catalyst-to-volume ratio of 1:20 in just 5 min using 20 mM H_2O_2 as oxidant. Phenomenal improvement in catalyst efficiency can be attributed to Fe-Schiff's base modification. Details of the contribution of various parameters on the catalytic performance of LDH and modified LDH are given below.

Table 2. The porosity data of LDH and Fe(III)SB-LDH obtained by nitrogen adsorption porosimetry.

Sample name	Surface area (m^2/g)	Pore diameter (nm)	Pore volume (cc/g)
LDH	3.059	17.548	0.007
MLDH	6.561	4.728	0.003

It is known that the Fenton type reactions which utilize a catalyst and H_2O_2 are pH-dependent [27]. In this study, we examined the impact of pH on the degradation of 4-NP using LDH and Fe(III)SB-LDH/H_2O_2 system across a pH range of 2–10. The results displayed in Fig. 7a indicate that the degradation efficiency for LDH and Fe(III)SB-LDH is 99% at pH 2. It is noteworthy that for LDH, the degradation efficiency improves at pH 2 but then declines drastically at 8 and 10, with values of 42% and 26%,

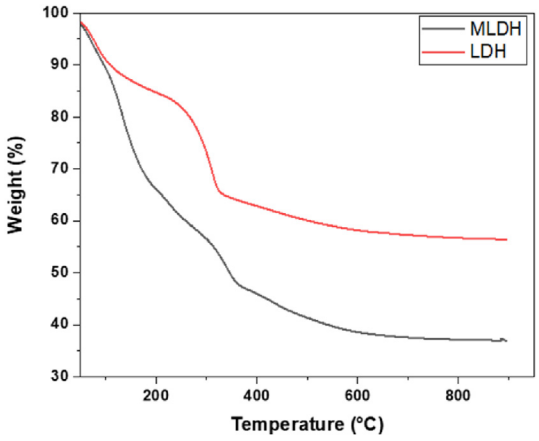

Fig. 6. TGA and DTA curve of LDH and Fe(III)SB-LDH.

respectively. However, for Fe(III)SB-LDH, the degradation efficiency does not decline abruptly. Similar studies are reported by Nguyen *et al.* on NiCo-LDH which exhibited high efficiency for the degradation of RhB dye, achieving a degradation rate of up to 96.7% in both acidic and neutral environments. However, its performance significantly declined in a basic environment, dropping to 69.6% [28]. The findings align with other studies as well [29,30]. In previous studies, Jawad *et al.* observed a degradation efficiency of 98% for phenol at a broad pH range of 5–12 [31] using copper nanoparticles and LDH composite catalysts.

This indicates that LDH not only hosts the active materials but also changes the microenvironment and pH-dependent activity of the catalysts. The degradation of 4-nitrophenol (4-NP) at different concentrations (2.5, 5, 10, 20 and 25 mg/L) of 4-NP were optimized. As shown on Fig. 7b, Fe(III)SB-LDH can degrade 4-NP up to 99% at 10 μg/mL concentration in 5 min. However, the degradation efficiency decreases by increasing the concentration to 79% at 20 μg/mL and 72% at 25 μg/mL. It is because when the excess amount of 4-NP reacts with a fixed number of free radicals/active sites, the increasing

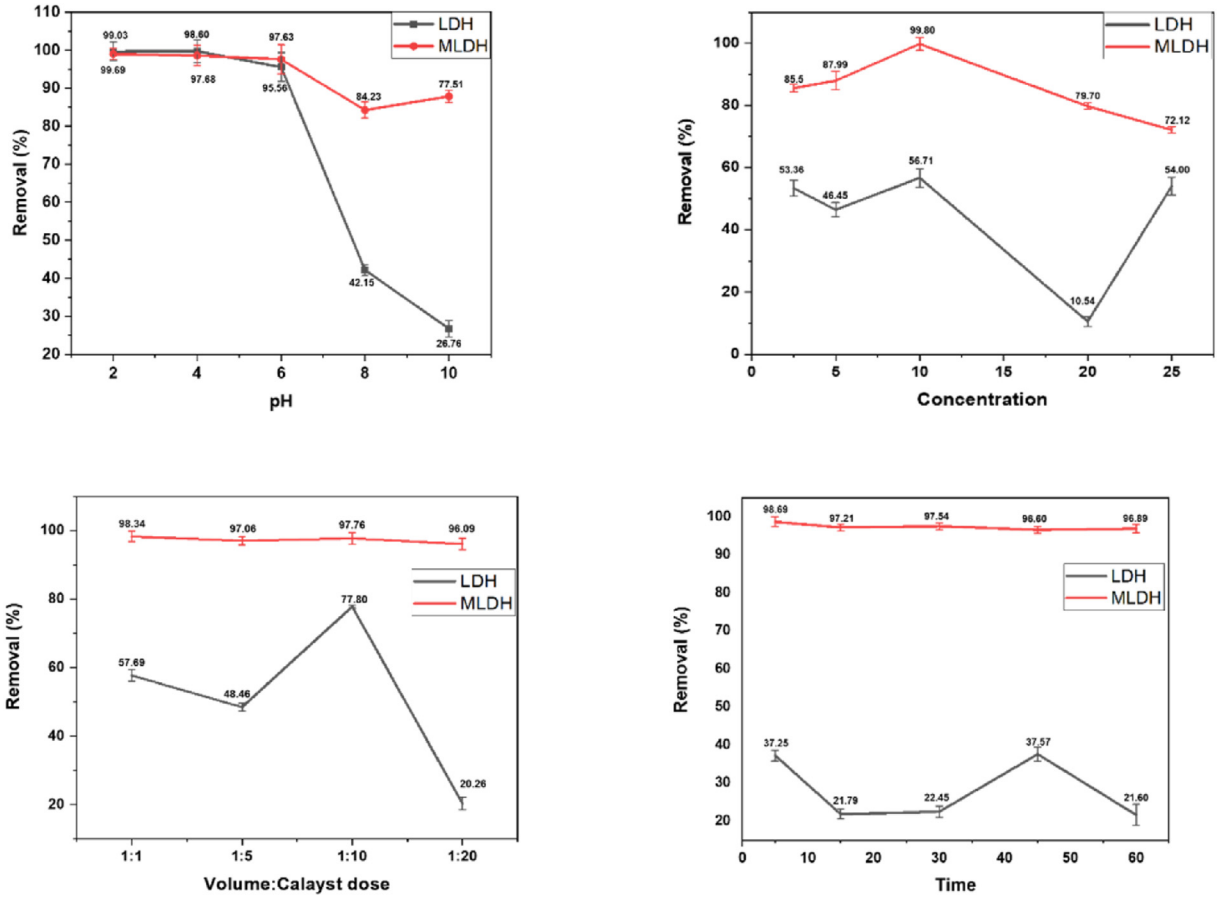

Fig. 7. Influence of pH on degradation efficiency of 4-NP (Conc: = 10 mg/L, H_2O_2 (20 mM) = 5 mL, shaking time = 10min. T = 30 °C) (a); Influence of concentration on degradation efficiency of 4-NP by LDH and Fe(III)SB-LDH (H_2O_2 (20 mM) = 5 mL, shaking time = 10min. T = 30 °C) (b); Influence of Solution volume: catalyst dose on degradation efficiency of 4-NP (Conc: = 10 mg/L, H_2O_2 (20 mM) = 5 mL, shaking time = 10min. T = 30 °C) (c) and; Influence of time (min) on degradation efficiency of 4-NP (Conc: = 10 mg/L, H_2O_2(20 mM) = 5 mL, T = 30 °C) (d).

competition between 4-Np and free radicals negatively affects the degradation efficiency of Fe(III)SB-LDH.

The performance of LDH and Fe(III)SB-LDH were also investigated using a ratio of volume (mL) to different amounts of catalyst (mg) (1:1 (10 mL:10mg/0.01g), 1:5 (10 mL:50mg0.05g), 1:10 (5 mL:50mg/0.05g) and 1:20 (10 mL:200mg/0.2g)) at fixed amount of H_2O_2 (20 mM) (Fig. 7c). The results showed that Fe(III)SB-LDH at 1:1 has higher degradation efficiency than LDH and the degradation of 4-NP to 98% in 5 min. From the results of Fe(III)SB-LDH, it is shown that the degradation efficiency is in equilibrium, the competitive consumption of radicals may cause adverse effects, and with excess amount of catalysts and diffusion limitation phenomenon [32,33]. The results showed that H_2O_2 without a catalyst could only give a degradation efficiency of 36.82% of 4-NP. The effect of reaction time (5, 15, 30, 45, and 60 min) on LDH and Fe(III)SB-LDH/H_2O_2 was shown in Fig. 7d. The higher degradation efficiency i.e., 98% of 4-NP achieved in 5 min by Fe(III) SB-LDH and gets equilibrium.

3.3.1. Degradation products of 4-NP using Fe(III)SB-LDH catalyst

An oxidative pathway for 4-NP by a process can be suggested based on the identification of intermediates. There are two different ways that 4-NP can be initially oxidized. In the first route, NO_2 is released during the formation of hydroquinone and 1,2,4 trihydroxylbenzene, which is then followed by ring cleavage oxidation to produce nitrogen-free small molecule compounds. The second process involves the formation of 4-nitrocatechol and 4-nitropyrogallol, which are then subjected to ring cleavage oxidation to produce certain nitrogenous chemicals. It should be noted that hydroquinone and benzoquinone are in equilibrium in aqueous solution [34,35]. In addition, when hydroxyl radicals are present, hydroquinone is easily converted to benzoquinone which may therefore function as an intermediary in the degradation of 4-NP. Furthermore, when a hydroxyl radical hits various locations on the benzene ring and initiates various oxidation pathways, hydroxylated molecules of 4-NP are created. In the presence of the electron-donor group, OH in the benzene ring at the ortho- and para-positions of 4-NP are vulnerable to attack by the electrophilic reagent $^{\bullet}OH$. Henceforth, when $^{\bullet}OH$ radicals interact with 4-NP, reactions are set off that result in hydroxylated compounds via denitration or an H-abstraction process. Because the NO_2 group is easily removed, 4-NP will easily oxidize to hydroquinone with the removal of the nitro group occurring simultaneously. The subsequent oxidation of hydroquinone results in the formation of 1,2,4-trihydroxybenzene as well, which is then followed by ring cleavage and final mineralization. In addition to free radical derived degradation, an alternate mechanism for degradation of phenol involving singlet oxygen species ($^1O_2$) is also reported [36]. The $^1O_2$ is produced using bimetallic Mo and Ni Co-doped g C_3N_4 composite catalyst where reaction proceeds as Fenton-like degradation process promoted by non-free radical $^1O_2$. The reaction showed high degradation efficiency in a wide pH range. The formation of $^1O_2$ in the presence of Fe(III) Schiff base complex and H_2O_2 is also reported [37].

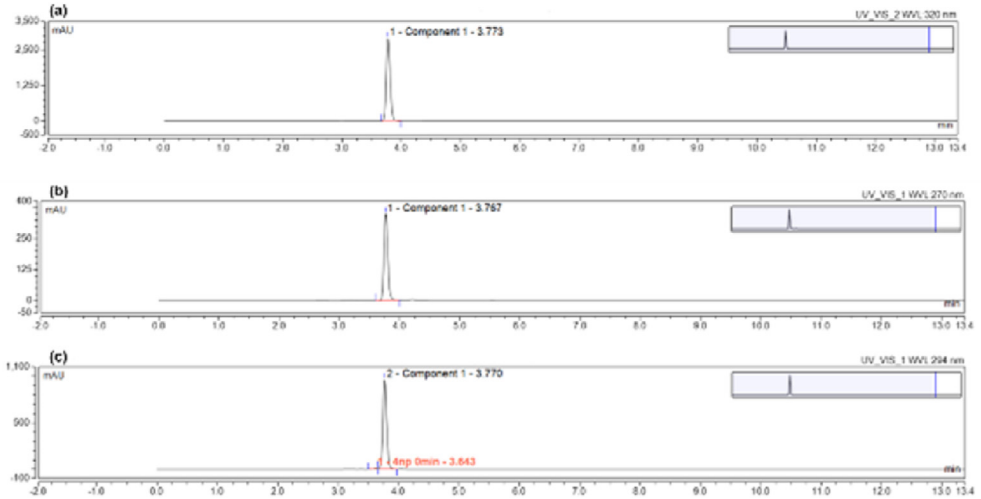

Fig. 8. UPLC chromatogram of 4-nitrophenol solution without treatment (a) and after treatment with Fe-(III) SB-LDH catalytic system (b and c) degradation.

To understand the degradation mechanism in this study, the reaction products were identified by running the standard 4-nitrophenol and the reaction mixture after oxidation on HPLC connected with a diode array detector. Fig. 8a shows the chromatogram 4-nitrophenol at a detection wavelength of 320 nm where the peak was observed at 15 min elution time. After adding Fe(III)SB-LDH, no peak was observed at t_R of 3.77 min at 320 nm but two peaks appear at 270 and 294 nm which correspond to peak maxima of 1,2,4-trihydroxy benzene and benzoquinone [38,39]. Therefore, it may be suggested that 4-nitrophenol is converted to these two products. Henceforth, it may be safely assumed that the reaction is Fenton-like in nature. However, more studies are needed to confirm the pathway for the degradation of 4-nitrophenol.

3.4. Catalytic reusability

It is important to know the stability of heterogeneous catalysts for possible repeated applications. To address this issue, reaction cycle tests were performed. At the end of every run Fe(III)SB-LDH was filtered, washed, and reused. 4-NP removal dropped in fourth run to 78% for Fe(III)SB-LDH (Fig. 9). Recovery amount of Fe(III)SB-LDH after every run is shown in Table 3 which shows that catalyst loss of Fe(III)SB-LDH after reusing reaches 20% on fifth cycle. This shows that loss of efficiency in the catalytic degradation of nitrophenol may be due to the loss of the catalyst during use-filter-use cycles and not due to inaccessibility or active sites.

3.5. Leaching from catalyst

Leaching is the process by which the active components of a solid material are released and transferred into a liquid medium, leaching to the eventual deactivation of the catalyst. The leaching of active phases poses significant challenges due to its irreversible nature, making it a major contributor to catalyst deactivation in liquid environments. As Fe(III)SB-LDH is layered within LDH there may be the chance of leaching. Therefore, it is important to check the leaching of components from catalysts. Henceforth, possible leaching of composited Fe(III)-Schiff's from composited catalyst was carried out by taking UV–Vis spectra of its aqueous extract and compared with solution pure Fe(III)-SB. the absence of a peak in aqueous extract indicated that there is no leaching of Schiff's base from Fe(III)SB-LDH. This observation provides evidence that no harmful substances were released during the reaction.

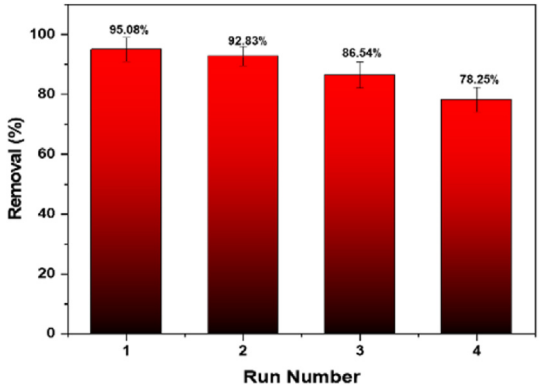

Fig. 9. Reusability graph for Fe(III)SB-LDH 4-NP (3.0 g of Fe(III)SB-LDH, Conc: = 25 mL (10 mg/L), H_2O_2 (20 mM) = 25 mL, shaking time = 10min. T = 30 °C).

Table 3. Fe(III)SB-LDH reusability test and its recovery amount for 4-NP degradation.

Runs/Cycles	Fe(III)SB-LDH Amount/Yield (g)	Loss of catalyst (%)
Fresh	3.00	–
1st	2.97	1
2nd	2.73	9
3rd	2.42	19
4th	2.38	20

4. Conclusion

In this work, an environmentally friendly efficient catalyst based on a composite of Fe-Schiff's base and layered of double hydroxides of aluminum and nickel (hydrotalcite) has been successfully prepared. Fe(III) SB-modified LDH had a larger surface area and narrower pores, which led to enhanced catalytic efficiency. XRD analysis confirmed the crystalline, layered structure with rhombohedral symmetry, for modified LDH a decrease in interlamellar space was observed. 4-nitrophenol degradation of 99% was achieved within contact time of 5min. The composite showed better efficiency in the whole pH range which makes it suitable for real world applications.

Funding

The work does not involve any data that requires ethical approvals.

Acknowledgment

The authors are thankful to the Higher Education Commission (HEC), Islamabad, for providing funds under the NRPU program (No. 8100) to conduct this research work. The authors are also Thankful to the Scientific and Technological Research Council of Türkiye (Türkiye Bruslari) for funding students to conduct part of the work.

References

[1] J. Mittal, Recent progress in the synthesis of Layered Double Hydroxides and their application for the adsorptive removal of dyes: a review, J. Environ. Manag. 295 (2021) 113017, https://doi.org/10.1016/j.jenvman.2021.113017.

[2] A. Tsyganok, R.G. Green, J.B. Giorgi, A. Sayari, Non-oxidative dehydrogenation of ethane to ethylene over chromium catalysts prepared from layered double hydroxide precursors, Cat. Comm. 8 (2007) 2186–2193, https://doi.org/10.1016/j.catcom.2007.04.031.

[3] K. Parida, M. Sahoo, S. Singha, Synthesis and characterization of a Fe (III)-Schiff base complex in a Zn-Al LDH host for cyclohexane oxidation, J. Mol. Cat. A 329 (2010) 7–12, https://doi.org/10.1016/j.molcata.2010.06.010.

[4] L.-Y. Wang, G.-Q. Wu, D.G. Evans, Synthesis and characterization of a layered double hydroxide containing an intercalated nickel (II) citrate complex, Mat.Chem. Phy. 104 (2007) 133–140, https://doi.org/10.1016/j.matchemphys.2007.02.098.

[5] N.H. Gutmann, L. Spiccia, T.W. Turney, Complexation of Cu (II) and Ni (II) by nitrilotriacetate intercalated in Zn–Cr layered double hydroxides, J. Mat.Chem. 10 (2000) 1219–1224, https://doi.org/10.1039/A909902F.

[6] M. Kaneyoshi, W. Jones, Formation of Mg-Al layered double hydroxides intercalated with nitrilotriacetate anions, J. Mat. Chem. 9 (1999) 805–811, https://doi.org/10.1039/A808415G.

[7] D.E. De Vos, B.F. Sels, P.A. Jacobs, Heterogeneous enzyme mimics based on zeolites and layered hydroxides, J Cattech 6 (2002) 14–29, https://doi.org/10.1023/A:1015375306212.

[8] S. Bhattacharjee, K.-E. Jeong, S.-Y. Jeong, W.-S. Ahn, Synthesis of a sulfonato-salen-nickel (II) complex immobilized in LDH for tetralin oxidation, New J. Chem. 34 (2010) 156–162, https://doi.org/10.1039/B9NJ00314B.

[9] B. Choudary, T. Ramani, H. Maheswaran, L. Prashant, K. Ranganath, K.V. Kumar, Catalytic asymmetric epoxidation of unfunctionalised olefins using silica, LDH and resin-supported sulfonato-Mn (salen) complex, J Ad. Syn. Cat. Comm. 348 (2006) 493–498, https://doi.org/10.1002/adsc.200505427.

[10] K.C. Gupta, A.K. Sutar, Catalytic activities of Schiff base transition metal complexes, Coord. Chem. Rev. 252 (2008) 1420–1450, https://doi.org/10.1016/j.ccr.2007.09.005.

[11] S. Oprea, V.O. Potolinca, V. Oprea, L.I. Diaconu, Structure–properties relationship of the polyurethanes that contain Schiff base in the main chain, High Performance Polymers 32 (2020) 784–792, https://doi.org/10.1177/0954008319901152.

[12] A.R. Ibrahim, Preparation and Characterization of some transition metal complexes of bis Schiff Base Ligand, Int. J. Adv. Res. 3 (2015) 315–324. https://www.researchgate.net/publication/316564052.

[13] B.S. Marques, K. Dalmagro, K.S. Moreira, M.L. Oliveira, S.L. Jahn, T.A. de Lima Burgo, G.L. Dotto, Ca–Al, Ni–Al and Zn–Al LDH powders as efficient materials to treat synthetic effluents containing o-nitrophenol, J. Alloys Comp. 838 (2020) 155628, https://doi.org/10.1016/j.jallcom.2020.155628.

[14] S. Ma, C. Fan, L. Du, G. Huang, X. Yang, W. Tang, Y. Makita, K. Ooi, Intercalation of macrocyclic crown ether into well-crystallized LDH: formation of staging structure and secondary host– guest reaction, Chem. Mat. 21 (2009) 3602–3610, https://doi.org/10.1021/cm9007393.

[15] B.A. Andrade-Espinoza, G.G. Carbajal-Arizaga, S. Rivas-Fuentes, K. Nuño, J.B. Pelayo-Vázquez, J. Arratia-Quijada, Synthesis of organic-inorganic hybrid material with a synergistic interface as a release agent for free acid β-Hydroxy-β-Methyl butyrate, J. Nanomat. 2021 (2021) 1–12, https://doi.org/10.1155/2021/3060539.

[16] S. Iguchi, S. Kikkawa, K. Teramura, S. Hosokawa, T. Tanaka, Investigation of the electrochemical and photo-electrochemical properties of Ni–Al LDH photocatalysts, Phys. Chem. Chem. Phy. 18 (2016) 13811–13819, https://doi.org/10.1039/C6CP01646D.

[17] J. Wang, Y. Song, Z. Li, Q. Liu, J. Zhou, X. Jing, M. Zhang, Z. Jiang, In situ Ni/Al layered double hydroxide and its electrochemical capacitance performance, Ener, Fuels 4 (2010) 6463–6467, https://doi.org/10.1021/ef101150b.

[18] T.D. Nguyen, Q.T.P. Bui, H.Q.H. Phan, C.X. Thang, L.T.B. Le Tran, X. Tien, L.G. Bach, Synthesis and characterization of layered double hydroxides with divalent ions (Mg2+, Cu2+, Ca2+, Ni2+, Co2+, and Zn2+), J. Mat. Sci. Sur. Engg. 4 (2016) 488–491.

[19] M.A. Peck, M.A. Langell, Comparison of nanoscaled and bulk NiO structural and environmental characteristics by XRD, XAFS, and XPS, Chem. Mat. 24 (2012) 4483–4490, https://doi.org/10.1021/cm300739y.

[20] B.G.P. Bezerra, L. Bieseki, M.I.S. Mello, D.R.D. Silva, C.B. Rodella, S. Pergher, Memory effect on a LDH/zeolite A composite: an XRD in situ study, Materials 14 (2021) 2102, https://doi.org/10.3390/ma14092102.

[21] J. Ahn, M. Han, C.S.J.P.i. Ha, Preparation and characterization of polyimide/modified layered double hydroxide nanocomposites, Mat. Design 60 (2011) 271–278, https://doi.org/10.1002/pi.2939.

[22] M. Thommes, K. Kaneko, A.V. Neimark, J.P. Olivier, F. Rodriguez-Reinoso, J. Rouquerol, K.S. Sing, Physisorption of gases, with special reference to the evaluation of surface area and pore size distribution (IUPAC Technical Report), Pure Appl. Chem. 87 (2015) 1051–1069, https://doi.org/10.1515/pac-2014-1117.

[23] E.M. Seftel, M. Niarchos, N. Vordos, J.W. Nolan, M. Mertens, A.C. Mitropoulos, E.F. Vansant, P. Cool, LDH and TiO2/LDH-type nanocomposite systems: a systematic study on structural characteristics, Micropor. Mesopor. Mat. 203 (2015) 208–215, https://doi.org/10.1016/j.micromeso.2014.10.029.

[24] B.N. Narayanan, R. Koodathil, T. Gangadharan, Z. Yaakob, F. K. Saidu, S. Chandralayam, Preparation and characterization of exfoliated polyaniline/montmorillonite nanocomposites, Mat. Sci. Engg. B 168 (2010) 242–244, https://doi.org/10.1016/j.mseb.2009.12.027.

[25] D. Lee, K. Char, Thermal degradation behavior of polyaniline in polyaniline/Na+-montmorillonite nanocomposites, Poly. Degrad. Stab. 75 (2002) 555–560, https://doi.org/10.1016/S0141-3910(01)00259-2.

[26] M. Çelik, M. Önal, Intercalated polyaniline/Na-montmorillonite nanocomposites via oxidative polymerization, J. Pol. Res. 14 (2007) 313–317, https://doi.org/10.1007/s10965-007-9113-y.

[27] S.J. Hug, O. Leupin, Iron-catalyzed oxidation of arsenic (III) by oxygen and by hydrogen peroxide: pH-dependent formation of oxidants in the Fenton reaction, Environ. Sci. Technol. 37 (2003) 2734–2742, https://doi.org/10.1021/es026208x.

[28] N.T. Dung, B.M. Thuy, L.T. Son, L.V. Ngan, V.D. Thao, M. Takahashi, S. Maenosono, T.V. Thu, Mechanistic insights into efficient peroxymonosulfate activation by NiCo layered double hydroxides, J. Environ. Res. 217 (2023) 114488, https://doi.org/10.1016/j.envres.2022.114488.

[29] S. Wu, H. Li, X. Li, H. He, C. Yang, Performances and mechanisms of efficient degradation of atrazine using peroxymonosulfate and ferrate as oxidants, Chem. Engg. J. 353 (2018) 533–541, https://doi.org/10.1016/j.cej.2018.06.133.

[30] Y. Ji, C. Dong, D. Kong, J. Lu, New insights into atrazine degradation by cobalt catalyzed peroxymonosulfate oxidation: kinetics, reaction products and transformation mechanisms, J. Haz. Mat. 285 (2015) 491–500, https://doi.org/10.1016/j.jhazmat.2014.12.026.

[31] A. Jawad, J. Lang, Z. Liao, A. Khan, J. Ifthikar, Z. Lv, S. Long, Zhulei Chen, Zhuqi Chen, Activation of persulfate by CuOx@ Co-LDH: a novel heterogeneous system for contaminant degradation with broad pH window and controlled leaching, Chem. Engg. J. 335 (2018) 548–559, https://doi.org/10.1016/j.cej.2017.10.097.

[32] X. Zou, T. Zhou, J. Mao, X. Wu, Synergistic degradation of antibiotic sulfadiazine in a heterogeneous ultrasound-enhanced Fe0/persulfate Fenton-like system, Chem. Engg. J. 257 (2014) 36–44, https://doi.org/10.1016/j.cej.2014.07.048.

[33] T. Zhang, H. Zhu, J.-P. Croue, Production of sulfate radical from peroxymonosulfate induced by a magnetically

separable CuFe2O4 spinel in water: efficiency, stability, and mechanism, Environ. Sci. Technol. 47 (2013) 2784–2791, https://doi.org/10.1021/es304721g.
[34] M.A. Oturan, J. Peiroten, P. Chartrin, A. Acher, Complete destruction of p-nitrophenol in aqueous medium by electro-Fenton method, Environ. Sci. Technol. 34 (2000) 3474–3479, https://doi.org/10.1021/es990901b.
[35] E. Lipczynska-Kochany, Degradation of nitrobenzene and nitrophenols by means of advanced oxidation processes in a homogeneous phase: photolysis in the presence of hydrogen peroxide versus the Fenton reaction, Chemosphere 24 (1992) 1369–1380, https://doi.org/10.1016/0045-6535(92)90060-5.
[36] Q. Song, W.-h. Ma, M.-k. Jia, D. Johnson, Y.-p. Huang, Degradation of organic pollutants in waters by a water-insoluble iron (III) Schiff base complex, Appl. Cat. A 505 (2015) 70–76, https://doi.org/10.1016/j.apcata.2015.07.028.
[37] M. Tian, X. Ren, S. Ding, N. Fu, Y. Wei, Z. Yang, X. Yao, Effective degradation of phenol by activating PMS with bimetallic Mo and Ni Co-doped g C3N4 composite catalyst: a Fenton-like degradation process promoted by non-free radical 1O2, Environ. Res. 243 (2024) 117848, https://doi.org/10.1016/j.envres.2023.117848.
[38] B. Philipp, B. Schink, Evidence of two oxidative reaction steps initiating anaerobic degradation of resorcinol (1, 3-dihydroxybenzene) by the denitrifying bacterium Azoarcus anaerobius, J. Bacteriol. 180 (1998) 3644–3649, https://doi.org/10.1128/jb.180.14.3644-3649.1998.
[39] S. Base. (09/09/2023). 1,2,4-Benzenetriol. Available: https://spectrabase.com/spectrum/D601OfpeLHe.